Ultrabroadband coherent supercontinuum frequency comb

Axel Ruehl,[1,*] Michael J. Martin,[2] Kevin C. Cossel,[2] Lisheng Chen,[2] Hugh McKay,[1] Brian Thomas,[1] Craig Benko,[2]
Liang Dong,[1,†] John M. Dudley,[3] Martin E. Fermann,[1] Ingmar Hartl,[1] and Jun Ye[2]

[1]*IMRA America Inc., 1044 Woodridge Avenue, Ann Arbor, Michigan 48105, USA*

[2]*JILA, National Institute of Standards and Technology and University of Colorado, Department of Physics, 440 UCB,
Boulder, Colorado 80309, USA*

[3]*Institute FEMTO-ST, CNRS-University of Franche-Comté UMR 6174, Besançon, France*

We present detailed studies of the coherence properties of an ultrabroadband supercontinuum, enabled by a comprehensive approach involving continuous-wave laser sources to independently probe both the amplitude and phase noise quadratures across the entire spectrum. The continuum coherently spans more than 1.5 octaves, supporting Hz-level comparison of ultrastable lasers at 698 nm and 1.54 μm. We present a complete numerical simulation of the accumulated comb coherence in the limit of many pulses, in contrast to the single-pulse level, with systematic experimental verification. The experiment and numerical simulations reveal the presence of quantum-seeded broadband amplitude noise without phase coherence degradation, including the discovery of a dependence of the supercontinuum coherence on the fiber fractional Raman gain.

Highly spatially and temporally coherent supercontinua (SC)-based optical frequency combs have applications ranging from broadband spectroscopy with high sensitivity and accuracy [1] to the spectral dissemination of optical frequency references, where coherently linking the visible spectrum to the telecom band is crucial for long-haul optical carrier transfer [2]. Additionally, and most importantly, highly phase coherent frequency combs directly impact the field of optical frequency standards, where the SC generated with phase-stabilized frequency combs allow comparison of optical frequency standards hundreds of THz apart [3]. Currently, the thermal noise-limited frequency stability of continuous-wave (CW) cavity-stabilized lasers sets a limit to the frequency stability of these optical standards, especially to those based on trapped ensembles of neutral atoms [4]. A direct spectral link between the 1.5 μm and visible spectral regions allows novel ultrastable laser systems operating in the telecom band [5] to be used as the local oscillators for current optical standards. A direct comb-based approach offers more complete spectral coverage and can circumvent frequency doubling of the CW laser or frequency comb, which adds non-common-path noise in addition to complexity.

In this Rapid Communication, we present a new method for verifying supercontinuum optical coherence, which allows us to conclusively demonstrate a spectrum that directly and coherently spans from the visible to the telecom band. This technique, applied to an ultrabroadband spectrum 1.5 octaves wide, utilizes optical heterodyne beat experiments and numerical simulations. This powerful combination has allowed us to identify regions of significant quantum-seeded amplitude noise that are decoupled from the phase noise of the continuum, proving that the comb phase coherence is preserved across the entirety of the 1.5-octave spectral range. In concert with

numerical simulations, we have reached an understanding of the important role that fiber Raman gain plays in maintaining broadband optical coherence in the supercontinuum.

The frequency comb used to generate the supercontinuum is based on a Fabry-Perot-type Yb-similariton oscillator mode locked with a sub-ps lifetime saturable absorber mirror [6]. While it has been demonstrated that fiber oscillators can produce high-quality frequency combs with excellent passive stability [7], pulse durations in the 100-fs range make it challenging to realize supercontinua with a high degree of coherence over a large spectral region [8], as the sensitivity of the broadening process to noise can lead to large fluctuations [9]. Therefore, we took careful steps to reach near transform-limited nJ-level pulses suitable for SC generation. The 152-MHz-pulse train was amplified in a Yb-doped double-clad phosphosilicate fiber with a 12-μm-core diameter pumped at 976 nm. To avoid self-phase modulation and hence to minimize amplitude-to-phase noise conversion in the fiber amplifier, a linear chirped-pulse amplification scheme was chosen, and it has been demonstrated that this amplification scheme is compatible with low-noise phase control [10]. With additional fiber-based compensation for higher-order dispersion contributions, the pulses could be recompressed to <80 fs with a grating compressor as characterized by frequency-resolved optical gating. We coupled the 1.2-nJ-pulse train to a highly nonlinear suspended core fiber [11] with a zero dispersion wavelength tuned to approximately 950 nm in order to optimize the spectrum, which spanned from 570 nm up to 1.66 μm at the −30-dB level as shown in Fig. 1(a). We note that the measured spectrum exhibits excellent agreement with the simulation [dashed line in Fig. 1(a)], which we later discuss in detail.

In order to test the phase coherence of the supercontinuum in different spectral regions, we performed free-running beat experiments with several CW lasers. Amplitude noise was identified with the help of dual-balanced detection, which cancels out common mode noise [12]. We implemented this scheme to obtain beat notes at 698 and 1020 nm, respectively (shown in Fig. 1) with a signal-to-noise ratio (SNR) of >30 dB at a 100-kHz resolution bandwidth (RBW). As shown

_____

*Present address: Institute for Lasers, Life and Biophotonics, Vrije Universiteit Amsterdam, The Netherlands; aruehl@few.vu.nl

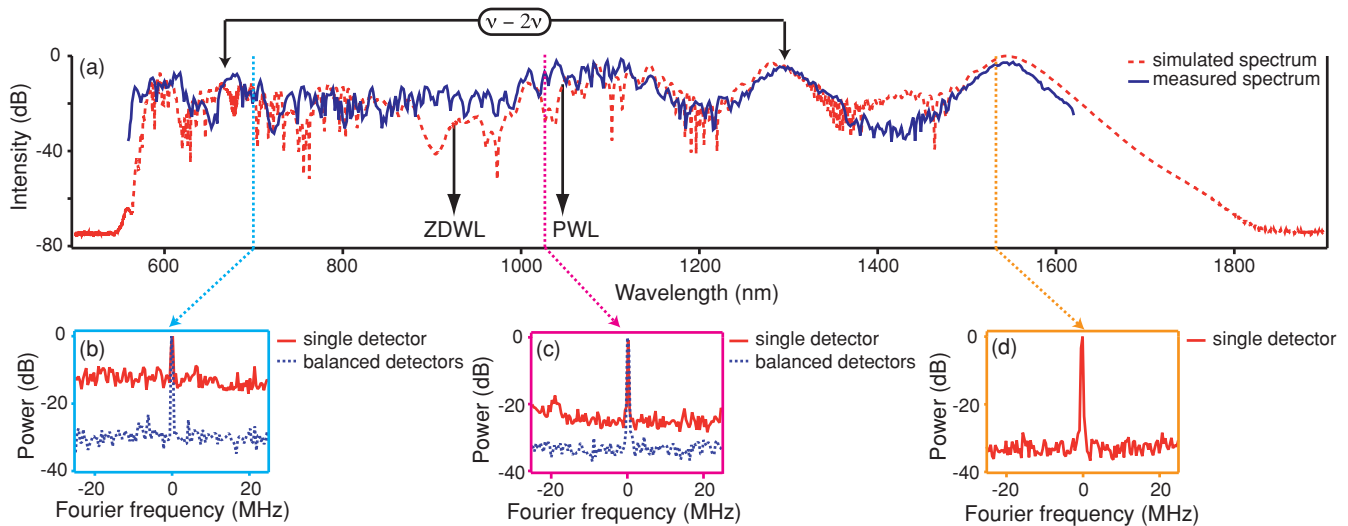†Present address: COMSET/ECE, Clemson University, Clemson, SC 29625.

FIG. 1. (Color) (a) Simulated (dashed line) and measured (solid line) solid supercontinuum spectrum at the output of the suspended core fiber. The zero dispersion wavelength (ZDWL) and pump wavelength (PWL) are shown with arrows. The self referencing $\nu - 2\nu$ interferometer wavelengths used in this work are also indicated. (b) Beat at 698 nm with (dashed line) and without (solid line) balanced detection. Up to 20 dB suppression of the amplitude noise floor is observed. (c) Beat at 1020 nm with (dashed line) and without (solid line) balanced detection. (d) Beat at 1.5 μm without balanced detection, exhibiting a signal-to-noise ratio comparable to that of the balanced cases.

in Figs. 1(b) and 1(c), the amplitude noise floor could be suppressed by up to 20 dB at 698 nm and 8 dB at 1020 nm by using dual-balanced detection compared to the measurement with a single detector. This observation supports the discovery of broadband amplitude noise of the comb without the presence of phase noise in these spectral regions. In other spectral regions (e.g., at 1540 nm) we observed that dual-balanced detection was not necessary to obtain a similar SNR [shown in Fig. 1(d)]. More than 30 dB SNR was also obtained for beat signals at 771 nm and for the $\nu - 2\nu$ heterodyne beat signal representing the carrier-envelope offset frequency, f_0. Self-referencing the comb was possible with $c/\nu = 1150$ nm to $c/\nu = 1300$ nm (and the corresponding second harmonic, 2ν) providing the freedom to detect other beat notes in this region.

The free-running beat signals demonstrate that the SC is coherent beyond the 1-μs time scale, permitting coherent beats with high SNR to be observed across the entire spectrum. We additionally performed a precision test of the comb coherence between two distant spectral regions to probe the coherence at the 1-s time scale and demonstrate an important technological milestone: the direct and precise comparison of ultrastable lasers in the visible and telecom bands. The self-referenced frequency comb was locked to a sub-Hz linewidth optical local oscillator at 698 nm used in the JILA Sr optical lattice clock [13]. Then the fully stabilized comb was compared to a second stabilized CW laser system at 1.54 μm based on a compact and energy-efficient diode laser (Redfern Integrated Optics) with a free-running linewidth of <10 kHz. The optical power of the diode laser was enhanced with a low-noise Er-doped fiber amplifier capable of powers up to 300 mW. The laser was stabilized by injection current control to an ultrahigh finesse optical cavity based on an ultra low expansion (ULE) glass spacer and fused silica mirrors, with finesse of 180 000 and a linewidth of 23 kHz, using the Pound-Drever-Hall scheme. The simple and robust lock facilitated unattended operation over

many days with Hz-level short-term stability. The stabilized 1.54-μm laser light was delivered to the frequency comb via a noise-canceled fiber. The corresponding beat-signal between the frequency comb and the stabilized 1.54-μm CW laser measured at a 100-kHz RBW is shown in Fig. 2(a). The beat signal was further mixed down to 50 kHz and measured with a Fourier analyzer with a 1-Hz RBW. From this measurement, one can deduce a coherence time of >200 ms corresponding to >3×10^7 pulses from our 152-MHz-pulse train. A similar value was also found by fitting the time record of the out-of-loop beat note. As depicted in Fig. 2(c), a chirped sinusoidal fitting function of a characteristic time span of >200 ms could be successfully applied to the experimental data.
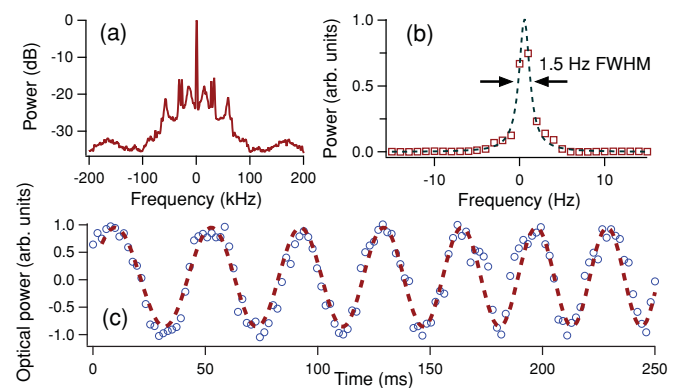

FIG. 2. (Color) Optical heterodyne beat results at 1.54 μm attained via comb-facilitated comparison of ultrastable lasers at 698 nm and 1.54 μm. (a) Broad (1-kHz RBW) and (b) narrow (1-Hz RBW) view of the resulting heterodyne beat at 1.54 μm (squares) and Lorenztian fit (dashed line). (c) Time domain representation of the heterodyne beat (circles) and fit (dashed line), demonstrating a coherence time of >200 ms. The fitting function is a chirped sine wave to account for relative linear drift between the two ultrastable lasers.

To better understand the spectral broadening process and SC coherence properties, we performed numerical simulations of the pulse dynamics within the nonlinear fiber. The propagation of the radially averaged electric field envelope, $A(z,t)$, is described by a generalized nonlinear Schrödinger equation [8,14],

$$\frac{\partial A(z,t)}{\partial z} - i\mathcal{F}^{-1}[(\beta(\omega) - \omega\beta_1 - \beta_0)\tilde{A}(z,\omega)]$$
$$= i\gamma\left(1 + \frac{i}{\omega_0}\frac{\partial}{\partial t}\right)\left[A(z,t)\int R(t')|A(z,t-t')|^2 dt'\right]. \quad (1)$$

The terms on the left side of the equation describe the contributions of the fiber dispersion to all orders while the terms on the right side take into account the relevant $\chi^{(3)}$ effects, namely, Raman scattering and the Kerr effect. Specifically, $\tilde{A}(z,\omega)$ is the Fourier transform of $A(z,t)$, $\mathcal{F}[A(z,t)]$; $\beta_k \equiv \frac{\partial^k}{\partial\omega^k}\beta(\omega)|_{\omega_0}$, where $\beta(\omega)$ is the propagation constant and ω_0 is the carrier frequency; γ is the nonlinear coefficient and is proportional to n_2, the nonlinear refractive index; and $R(t)$ is given by $R(t) = (1 - f_R)\delta(t) + f_R h_R(t)$. The Raman fraction, f_R, sets the ratio of Kerr to Raman nonlinearity; $h_R(t)$ is the time-domain Raman response [14]; and $\delta(t)$ is the Dirac δ function.

We measured the pulse energy coupled to the fiber (1.2 nJ), input spectrum, and fiber dispersion and used these as the basis for our simulation parameters. The input pulses were modeled as unchirped hyperbolic secant pulses of 80 fs in duration (full width at half maximum) with a center wavelength of 1050 nm. The fiber had a nonlinearity (γ) of approximately 40 W^{-1} km^{-1} and also an increased f_R, due to germanium doping, from the standard value of 0.18 for fused silica. We found that the simulated spectrum best matched the measured spectrum for $f_R = 0.28$ [Fig. 1(a)], consistent with the Raman gain increase observed in Ref. [15]. The injected soliton order [8], $N \simeq \sqrt{(0.5\gamma E_0 T_0)/|\beta_2|}$, where E_0 is the pulse energy and T_0 is the pulse duration, was 19.2.

In order to model quantum-limited SC coherence, we performed multiple simulations with a quantum shot noise seed perturbing the input pulse, $A(t)$, such that $A(t) \rightarrow A(t) + \Delta A(t)$. In this case, where the square modulus of A represents optical power, $\Delta A(t)$ is described stochastically by $\langle \Delta A^*(t)\Delta A(t + \tau)\rangle = (h\nu/2)\delta(\tau)$ [16,17], and we treat it as a Gaussian-distributed random variable in both quadratures. We also include the effects of spontaneous Raman scattering along the fiber according to the procedure of Ref. [16]. The first-order coherence, $g(\omega)$, defined as

$$g(\omega) = \frac{|\langle\tilde{A}_i(\omega)\tilde{A}_j^*(\omega)\rangle_{i\neq j}|}{\sqrt{\langle|\tilde{A}_i(\omega)|^2\rangle\langle|\tilde{A}_j(\omega)|^2\rangle}}, \quad (2)$$

was calculated numerically by an ensemble average over 100 independently simulated spectra according to Ref. [18], in 50-GHz spectral bins. Figure 3(a) shows $g(\omega)$ along with the calculated spectrum, and it can be seen that there are significant drops in the coherence in isolated spectral regions that still posses significant optical power. Another interesting note is that the coherence degrades smoothly across the first Raman soliton (with a corresponding increase in phase noise).

Numerically, we identified several parameters responsible for a significant loss of coherence. In particular, our quadrature-sensitive technique for measuring supercontinuum coherence led us to discover an interesting dependence on the fractional Raman contribution (f_R). We calculated the average coherence of the longest wavelength (first ejected) soliton and saw a decrease in coherence from 0.9 to 0.7 for f_R varying from 0.28 to 0.2 with the soliton center wavelength fixed by increasing the fiber length. The loss of coherence was most dramatic on the long-wavelength side of the soliton. We also noticed reduced coherence with increasing pulse energy and with increasing pulse duration (both increasing the soliton order) as has been observed in other studies [19]; however, we see a coupling between these parameters and f_R. With a higher value of f_R, the coherence was significantly less sensitive to pulse duration (slight loss of coherence in the soliton at 120 fs) and energy than with low values of f_R, where we saw strong loss of coherence in the first soliton and also low coherence across the spectrum with 90-fs pulses. These results are significant in that they demonstrate that intrapulse-stimulated Raman scattering plays a central role in generating supercontinuum spectra with high coherence. Specifically, although competition between noise amplification through modulation instability and coherent spectral broadening through soliton fission has already been identified as a key factor determining supercontinuum coherence, our results suggest that a higher fractional Raman contribution can mitigate the addition of noise to the propagating solitons. The increased rate at which the ejected solitons shift to longer wavelength reduces the detrimental effect of the modulation instability gain on the soliton amplitude and phase. Designing and fabricating fibers with higher fractional Raman contribution (e.g., higher Ge doping) may therefore represent an important technological tool for generating low-noise supercontinua, especially in cases where source parameters (pulse duration, power) cannot be independently controlled.

To better elucidate the experimental observations, we consider the different contributions to $g(\omega)$ arising from amplitude and phase noise separately [i.e., calculating the variance of the argument and amplitude of $\tilde{A}(\omega)$]. As evident in Fig. 3(b), it was numerically found that certain spectral regions feature decreased coherence arising from amplitude noise but exhibit only negligible phase noise contributions. The amplitude noise observed in the different spectral regions qualitatively agrees with the experimental trend observed in Fig. 1. Interestingly, and in relation to the previous discussion, the simulations show that the loss of coherence of the first soliton is due primarily to phase noise. This distinction between amplitude and phase contributions is in contrast to previous experimental studies, where SC coherence was demonstrated by the use of a modified Young experiment with two sources or delayed pulse interferometry, where such a clear distinction could not be made [20,21]. Furthermore, direct comparison between 1.54-μm and 698-nm CW lasers demonstrates the capability of delivering Hz-level (1-s level) optical linewidth (coherence time) across the whole optical spectrum and hence the connection of optical local oscillators at 1.5 μm to optical frequency standards. Supporting this experimental observation, numerical simulations of up to 1000 pulses show that the total phase standard deviation does
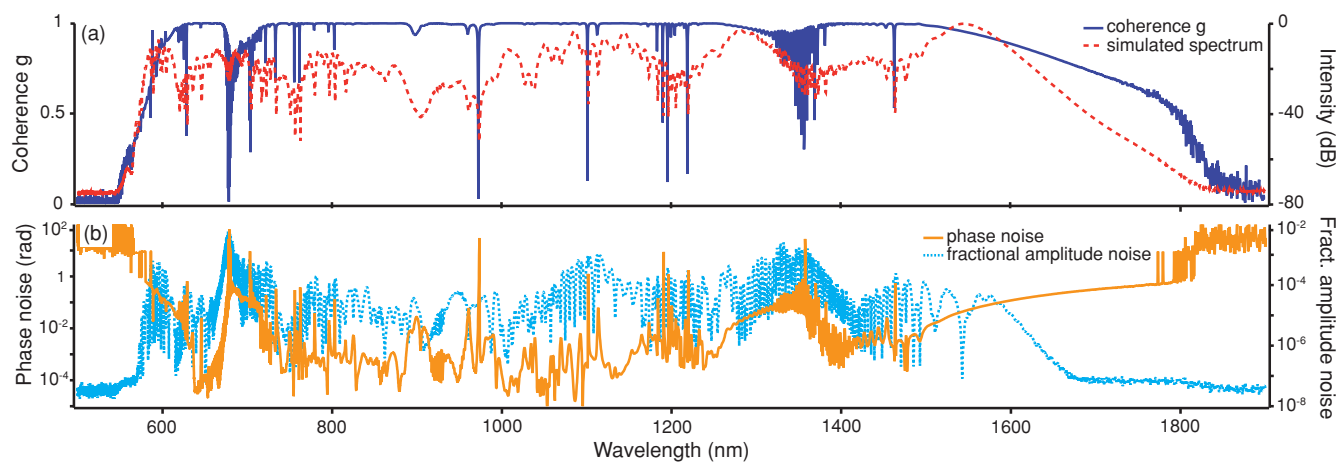
FIG. 3. (Color) Simulation results for the optical spectrum and coherence properties after broadening in the suspended core fiber. (a) Simulated spectrum (dashed line, right) and calculated quantum noise-limited pulse to pulse coherence (solid line, left). (b) Contributions of amplitude (dashed line, right) and phase (solid line, left) noise to the total coherence function. In many spectral regions, the presence of amplitude noise does not presage the presence of phase noise, indicating that degradation of $g(\omega)$ is not necessarily indicative of a loss of phase coherence.

not change, indicating that the quantum-noise-induced phase deviation is bound at some level and is not a random walk, which would degrade relative linewidth. This is consistent with other tests of comb coherence which reach the same conclusion [22]. SC generation can thus be seen as a white phase noise process without an accumulative component. This further confirms that the observed linewidth in the out-of-loop comparison was not compromised by the SC.

In conclusion, we have provided a systematic understanding of the coherence properties of a 1.5-octave-wide SC generated from an amplified Yb-fiber frequency comb via a new quadrature-sensitive technique utilizing CW laser sources. Contributions arising from amplitude and phase noise were experimentally observed and numerically confirmed. It was demonstrated that spectral regions with increased amplitude noise can still be utilized for high-quality optical phase measurements when dual-balanced detection is employed. We

identified relevant fiber parameters, crucially the fractional Raman contribution and its effect on soliton shifting rate, which will allow further improvement in the design of highly nonlinear fibers for optimized SC coherence properties. Importantly, we demonstrated coherence transfer over more than one octave between ULE cavity-stabilized diode lasers at $1.54\ \mu$m and 698 nm, representing the largest spectral gap directly spanned between two ultrastable lasers by a frequency comb to date. Limited by the linewidth of the 1.54-μm laser, a coherence time of >200 ms was found. This technique could enable more detailed and quantitative studies of SC coherence.

[1] I. Coddington, W. C. Swann, and N. R. Newbury, Phys. Rev. Lett. **100**, 13902 (2008); K. C. Cossel *et al.*, Appl. Phys. B1 (2010).

[2] O. Terra *et al.*, Appl. Phys. B **97**, 541 (2009).

[3] S. M. Foreman *et al.*, Phys. Rev. Lett. **99**, 153601 (2007).

[4] A. Quessada *et al.*, J. Opt. B: Quantum and Semiclassical Optics **5**, S150 (2003).

[5] F. Kéfélian, H. Jiang, P. Lemonde, and G. Santarelli, Opt. Lett. **34**, 914 (2009).

[6] I. Hartl, G. Imeshev, L. Dong, G. C. Cho, and M. E. Fermann, in *Conference on Lasers and Electro-Optics/Quantum Electronics and Laser Science and Photonic Applications Systems Technologies, Technical Digest (CD)* (Optical Society of America, 2005), paper CThG1 [http://www.opticsinfobase.org/abstract.cfm?URI=CLEO-2005-CThG1].

[7] N. R. Newbury and W. C. Swann, J. Opt Soc. Am. B **24**, 1756 (2007).

[8] J. M. Dudley, G. Genty, and S. Coen, Rev. Mod. Phys. **78**, 1135 (2006).

[9] M. Nakazawa, K. Tamura, H. Kubota, and E. Yoshida, Opt. Fiber Technol. **4**, 215 (1998).

[10] T. R. Schibli *et al.*, Nat. Photonics **2**, 355 (2008); A. Ruehl, A. Marcinkevicius, M. E. Fermann, and I. Hartl, Opt. Lett. **35**, 3015 (2010).

[11] L. Fu, B. K. Thomas, and L. Dong, Opt. Express **16**, 19629 (2008).

[12] H. P. Yuen and V. W. S. Chan, Opt. Lett. **8**, 177 (1983).

[13] A. D. Ludlow *et al.*, Opt. Lett. **32**, 641 (2007).

[14] K. J. Blow and D. Wood, IEEE J. Quantum Electron. **25**, 2665 (1989).

[15] F. A. Oguama, H. Garcia, and A. M. Johnson, J. Opt. Soc. Am. B **22**, 426 (2005).

[16] K. L. Corwin *et al.*, Phys. Rev. Lett. **90**, 113904 (2003).

[17] R. Paschotta, Appl. Phys. B: Lasers and Optics **79**, 153 (2004).

[18] J. M. Dudley and S. Coen, IEEE J. Quantum Electron. **8**, 651 (2002).

[19] A. Demircan and U. Bandelow, Appl. Phys. B **86**, 31 (2007).

[20] M. Bellini and T. W. Hänsch, Opt. Lett. **25**, 1049 (2000).

[21] F. Lu and W. Knox, Opt. Express **12**, 347 (2004).

[22] M. J. Martin, S. M. Foreman, T. R. Schibli, and J. Ye, Opt. Express **17**, 558 (2009).